Published in final edited form as:
*Development*. 2008 August ; 135(15): 2637–2648. doi:10.1242/dev.022244.

# Temporal Requirements of the Fragile X Mental Retardation Protein in the Regulation of Synaptic Structure

**Cheryl L. Gatto** and **Kendal Broadie**
Department of Biological Sciences, Kennedy Center for Research on Human Development, Vanderbilt University, Nashville, TN 37232 USA

## Abstract

Fragile X Syndrome (FraX), caused by the loss of function of one gene (FMR1), is the most common inherited form of both mental retardation and autism spectrum disorders. The FMR1 product (FMRP) is an mRNA-binding translation regulator that mediates activity-dependent control of synaptic structure and function. To develop any FraX intervention strategy, it is critical to define when and where FMRP loss causes the manifestation of synaptic defects, and whether reintroduction of FMRP can restore normal synapse properties. In the *Drosophila* FraX model, dFMRP loss causes neuromuscular junction (NMJ) synapse over-elaboration (overgrowth, overbranching, excess synaptic boutons), accumulation of development-arrested satellite boutons, and altered neurotransmission. We have used the Gene-Switch (GS) method to conditionally drive dFMRP to define the spatiotemporal requirements in synaptic mechanisms. Constitutive induction of targeted neuronal dFMRP at wild-type levels rescues all synaptic architectural defects in *dfmr1* null mutants, demonstrating a presynaptic requirement for synapse structuring. In contrast, presynaptic dFMRP expression does not ameliorate functional neurotransmission defects, indicating a postsynaptic dFMRP requirement. Strikingly, targeted early induction of dFMRP effects nearly complete rescue of synaptic structure defects, showing a primarily early development role. In addition, acute dFMRP expression at maturity partially alleviates *dfmr1* null defects, although rescue is not as complete as either early or constitutive dFMRP expression, showing a modest capacity for late-stage structural plasticity. We conclude that dFMRP predominantly acts early in synaptogenesis to modulate architecture, but that late dFMRP introduction at maturity can weakly compensate for early absence of dFMRP function.

### Keywords

*Drosophila*; gene-switch; neuromuscular junction; bouton; futsch

## Introduction

The Fragile X Syndrome (FraX) mental retardation and autism spectrum disorder, with a prevalence of ~1:4000 males and 1:6000 females, is among the most common inherited neurological diseases (Koukoui and Chaudhuri, 2007; Penagarikano et al., 2007). Loss of Fragile X Mental Retardation Protein (FMRP) expression is the sole cause of the disease state. FMRP is an mRNA-binding protein that regulates mRNA stability and translation for a number of synaptic and cytoskeleton-associated proteins (Castets et al., 2005; Lu et al., 2004; Muddashetty et al., 2007; Reeve et al., 2005; Todd et al., 2003; Zalfa et al., 2007; Zhang et al., 2001). FMRP function regulates the activity-dependent control of synaptic connections via

**Correspondence:** Kendal S. Broadie, Professor 6270 MRB III, 465 21st Avenue South Nashville, TN 37232 USA Tel: 615-936-3937 (office); -3935, -3936, and -6761 (lab); Fax: 615-936-0129 Email: kendal.broadie@vanderbilt.edu.

intersection with group 1 metabotropic glutamate receptor (mGluR) signaling (Antar et al., 2004; Bear et al., 2004; Ferrari et al., 2007; Huber et al., 2002; Nosyreva and Huber, 2006; Pan and Broadie, 2007; Pan et al., 2008). The synapsopathic clinical manifestations of the disease include mild to severe mental retardation (Penagarikano et al., 2007), delayed and depressed developmental trajectories (Bailey et al., 2001a; Bailey et al., 2001b), deficits in short-term memory (Cornish et al., 2001; Munir et al., 2000), hyperactivity (Einfeld et al., 1991), disordered sleep (Gould et al., 2000), seizures (Sabaratnam et al., 2001), and the cytological presentation of long, immature-looking cortical dendritic spines, indicating inappropriate development and/or failure of pruning and synapse elimination (Hinton et al., 1991; Rudelli et al., 1985).

Understanding FraX pathogenesis, and subsequently designing effective FraX interventions, requires knowledge of the temporal requirement(s) of FMRP function. A fundamental need is to determine whether FraX is primarily a `developmental disease', reflecting a transient role for FMRP in progressive neuronal maturation, a `plasticity disease', reflecting a maintained, constitutive requirement for FMRP at maturity, or some combination of a two-phase requirement giving rise to different FraX symptoms. This study aims to begin resolving this vital question using our well-characterized *Drosophila* FraX disease model (Zhang et al., 2001). Null *dfmr1* mutants are fully viable but display impaired learning and memory (Dockendorff et al., 2002), arrhythmic circadian motor activity (Dockendorff et al., 2002; Inoue et al., 2002), over-elaboration of neuronal structure (Michel et al., 2004; Morales et al., 2002; Pan et al., 2004; Zhang et al., 2001), and altered neuronal function (Zhang et al., 2001). The primary synaptic model is the neuromuscular junction (NMJ), which displays increased synapse arborization and branching, increased synaptic bouton number, and elevated neurotransmission. As in mammals, dFMRP functionally interacts with mGluR-mediated synaptic glutamatergic signaling in the regulation of postsynaptic glutamate receptor expression (Pan and Broadie, 2007) and in sculpting presynaptic architecture (Pan et al., 2008).

In this study, we use the conditional, transgenic Gene-Switch (GS) method (Osterwalder et al., 2001) to drive wild-type dFMRP expression in null *dfmr1* mutants. This approach allows targeted dFMRP expression during discrete temporal windows, enabling the definition of critical periods of function. We show that constitutive neuronal dFMRP expression rescues all NMJ synaptic structural defects, demonstrating a strictly presynaptic dFMRP requirement, with a mechanistic role in microtubule cytoskeleton regulation. In contrast, targeted presynaptic dFMRP expression does not rescue neurotransmission function in the null mutant, indicating a separable postsynaptic dFMRP requirement. Temporally, we show transient early-development expression of dFMRP strongly rescues all facets of synaptic architecture, demonstrating an early role for dFMRP in establishing synapse morphology. We also show that acute dFMRP expression at maturity weakly rescues a subset of synaptic structure defects, showing that dFMRP can mediate some structural plasticity and that late stage intervention may be beneficial.

## Materials and Methods

### Drosophila Genetics

Fly stocks were maintained at 25 °C on standard medium. The $w^{1118}$ line served as the genetic background control for the *dfmr1* null. Recombinant parental lines harboring the null *dfmr1* allele ($dfmr1^{50M}$) (Zhang et al., 2001) and either a wild-type *dfmr1* transgene under UAS control (UAS-9557-3) (Zhang et al., 2001) or the neuronal-specific driver *elav*-Gene-Switch construct (GSG-301) (Osterwalder et al., 2001) were generated using standard genetic techniques. Henceforth, “GS” as a genotype descriptor refers to the following: $dfmr1^{50M}$, *elav*-GSG-301/$dfmr1^{50M}$, UAS-9557-3. For RU486 (mifepristone; Sigma, St. Louis, MO)

dosing, the drug was dissolved in 80% ethanol (EtOH) and mixed with food to the desired concentration (shown in figures as GS+RX with RU486 in μg/mL). For vehicle control, the equivalent volume of EtOH was used to identically treat the GS line (GS+E). GS animals were either constitutively raised on supplemented/control food or transferred at staged times as indicated.

### Western Blot Analyses

The central nervous system (CNS), including the brain and the ventral nerve cord, was dissected free from staged and treated larvae in $Ca^{2+}$-free modified Jan's standard saline (Jan and Jan, 1976). Dissected CNS samples were homogenized and boiled in 1X NuPage sample buffer (Invitrogen, Carlsbad, CA) supplemented with 40 mM DTT. The total protein from 2-6 brains per sample (depending on larval age) was loaded onto 4-12% Tris-Bis gels and electrophoresed in NuPage MES Buffer (Invitrogen) for 1 hour at 200 V. Transfer to nitrocellulose was carried out for 1 hour at 100 V in NuPage transfer buffer (Invitrogen) + 10% MeOH. Processing was completed using the Odyssey near infrared fluorescence detection system (Li-COR, Lincoln, NE) to enable quantitative western blot analysis. Antibodies used included: anti-dFMRP (1:3000; 6A15 (monoclonal), Sigma), anti-α-tubulin (1:100,000; B512 (monoclonal), Sigma), and Alexagoat-anti-mouse-680 (1:10,000; Invitrogen-Molecular Probes). Raw integrated intensities were calculated for dFMRP for the lower molecular weight band of the doublet and α-tubulin band. The ratio of dFMRP:α-tubulin normalized for loading.

### Immunohistochemistry

Staged animals were dissected in standard saline and then fixed for 40 minutes with 4% paraformaldehyde/4% sucrose in phosphate buffered saline (PBS), pH 7.4. Preparations were rinsed with PBS, then blocked and permeablized with 0.2% triton X-100 in PBS (PBST) + 1% bovine serum albumin (BSA) + 0.5% normal goat serum (NGS) for 1 hour at room temperature. Primary and secondary antibodies were diluted in PBST + 0.2% BSA + 0.1% NGS and incubated overnight at 4°C and 2 hours at room temperature, respectively. Antibodies employed include: anti-dFMRP (1:500; 6A15), anti-DLG (1:200; 4F3 (monoclonal), Developmental Studies Hybridoma Bank (DSHB), Univeristy of Iowa), anti-Futsch (1:200; 22C10 (monoclonal), DSHB), anti-HRP (1:250; (polyclonal), Sigma), and Alexa-Fluor secondaries (1:250; Invitrogen-Molecular Probes). All fluorescent images were collected using a ZEISS LSM 510 META laser scanning confocal microscope.

### Synaptic Structure Analyses

The muscle 4 NMJ of abdominal segment 3 was used for all quantification. Values were determined for both left and right hemisegments; averaged for each n=1. Synapse junctional area was measured as the maximal cross-sectional area in a maximum projection of each collected Z-stack. A synaptic branch was defined as an axonal projection with at least 2 synaptic boutons. Two bouton classes were defined; 1) type Ib (>2 μm diameter) and 2) mini/satellite (≤2 μm diameter and attached to a type Ib bouton of mature size). Each class is reported as number per terminal. ImageJ (http://rsb.info.nih.gov/ij/) was used for fluorescence intensity thresholding, automated regional outline and area calculation.

### FM1-43 Assays

Staged animals were dissected in standard saline (+0.2 mM $CaCl_2$). NMJ preparations were loaded with FM1-43 (10 μM; Invitrogen-Molecular Probes) using depolarizing 90 mM KCl standard saline (+1.8 mM $CaCl_2$) for 5 minutes, washed and imaged. Preparations were then unloaded with the same stimulation for 2 minutes in the absence of FM1-43, washed and imaged. For quantification, only the muscle 4 NMJ in abdominal segments A2-A4 was used. Average fluorescence intensity values and bouton areas were measured from 3 NMJs per

animal, with 6 individual boutons per NMJ assayed, and then averaged to generate a single data point (n=1 from 18 boutons). The fluorescence intensity units (FIU) measured per bouton are shown, together with the ratio of FM1-43 unload:load fluorescence intensity.

### Electrophysiology

Two-electrode voltage-clamp recordings were made at 18°C from muscle 6 in abdominal segments A2-A4 of wandering 3rd instars to examine miniature excitatory junctional currents (mEJCs) (Zhang et al., 2001). Borosilicate glass electrodes were filled with 3 M KCl in standard saline containing (in mM): 128 NaCl, 2 KCl, 4 $MgCl_2$, 70 sucrose, 5 HEPES, and 0.2 $CaCl_2$. Tetrodotoxin (3 μM; Sigma) was added to block action potentials. Each n=1 results from 240 seconds of gap-free recording from independent animals. Traces were filtered using a low-pass 8-pole Bessel filter with -3 dB cutoff of 0.5 kHz. Data were analyzed using Clampfit 9.2 (Molecular Devices, Sunnyvale, CA) using template-based event detection. All traces were analyzed for mean peak amplitude (nA) and frequency (Hz).

### Statistics

Statistical analysis was done using GraphPad InStat 3 (GraphPad Software, Inc., San Diego, CA). Generally, unpaired t-tests were used to compare means of control and *dfmr1*, and Tukey-Kramer multiple comparisons tests were applied to all GS categories. In FM1-43 experiments, Dunnet's multiple comparison tests were also used to compare each value independently to the stated control. Significance levels in figures are represented as $p<0.05$ (*); $p<0.01$ (**); $p<0.001$ (***). All error bars represent standard error of the mean (s.e.m.).

## Results

### Targeted conditional expression of dFMRP in the nervous system

The conditional Gene-Switch (GS) method utilizes a modified UAS-GAL4 system that provides a means of tightly regulating tissue-specific transgene expression in order to define spatiotemporal requirements (McGuire et al., 2004; Osterwalder et al., 2001). GS-GAL4 lines are dependent on the progesterone analog RU486 (mifepristone) to drive hormone-responsive UAS-construct expression (Fig. 1A). We have driven a UAS-*dfmr1* transgene with neuronal *elav*-GS GAL4 in the *dfmr1* null mutant background to determine spatial and temporal requirements for dFMRP at the NMJ synapse. Thus, we assayed, in a targeted fashion, the presynaptic roles of dFMRP in synapse assembly and function following constitutive expression and timed intervention windows.

The critical first step was to determine RU486 dosage sufficient to match dFMRP levels in wild-type, so that the transgenic protein is not under- or over-expressed. RU486 dosage dependence tests were conducted by assaying dFMRP expression in the larval CNS by western blot (Fig. 1B, C) and immunohistochemistry *in situ* (Fig. 1D). Analyses were performed on wild-type control ($w^{1118}$), *dfmr1* null and *dfmr1* null animals harboring both the *elav*-GS GAL4 driver and UAS-*dfmr1* transgene (GS animals, henceforth), with RU486 (GS+R) or only ethanol vehicle (GS+E) constitutively fed. RU486 fed at 0.5 μg/mL yields dFMRP levels closely approximating wild-type control (98±5%), whereas RU486 at 1-2 μg/mL induce progressive over-expression (190±32% and 255±25% compared to control, respectively; 2 μg/mL vs. control, $p<0.05$; Fig. 1C). Thus, in GS animals, RU486 drives dose-dependent expression of dFMRP in the nervous system, and the dosage of 0.5 μg/mL fed constitutively generates dFMRP expression indistinguishable from wild-type.

### Presynaptic dFMRP expression rescues *dfmr1* null synapse architecture

In the *Drosophila* FraX model, loss of dFMRP causes NMJ over-elaboration (including excessive branching, overgrowth and supernumerary synaptic boutons), accumulation of mini- or satellite boutons, and altered functional neurotransmission properties due to both pre- and postsynaptic defects (Zhang et al., 2001). To quantify branching, individual projections harboring >2 boutons were counted as synaptic branches (control: 3.0±0.3 branches vs. *dfmr1*: 4.8±0.2 branches, n=12, p<0.001; Fig. 2A,B). To quantify synaptic area, the junction was delimited by either HRP (presynaptic) or DLG (postsynaptic) and area measured (ex. HRP - control: 160±8 $\mu m^2$ vs. *dfmr1*: 241±12 $\mu m^2$, n=12, p<0.001; Fig. 2C, D). Lastly, type Ib bouton numbers per terminal were counted, partitioned into either mature boutons (control: 19 ±1 boutons vs. *dfmr1*: 29±1 boutons, n=12, p<0.001; Fig. 2F) or mini/satellite boutons based on size and relative positioning (control: 0.6±0.2 mini-boutons vs. *dfmr1*: 3.7±0.4 mini-boutons, n=12, p<0.001; Fig. 2E, G).

We tested for rescue of architectural defects with constitutive presynaptic dFMRP induction. NMJs were double-labeled with anti-HRP, to delineate the innervating presynaptic neuron, and anti-DLG to reveal the postsynaptic domain of the target muscle (Fig. 2A). GS animals fed vehicle (EtOH) fully phenocopy the *dfmr1* null with respect to all structural abnormalities (Fig. 2). In sharp contrast, constitutively RU486-fed animals are completely rescued with entirely normal synaptic architecture. Presynaptically targeted dFMRP was assayed with two RU486 dosages: 0.5 μg/mL (wild-type dFMRP level; Fig. 1C) and 2.0 μg/mL (significantly elevated dFMRP; Fig. 1C). As predicted, the wild-type control matched dFMRP expression provides the most exact rescue of synaptic structure features. First, synaptic branch number was perfectly rescued from the elevated branching characterizing the null mutant (GS+E: 4.5 ±0.3 branches vs. GS+RU486 0.5 μg/mL: 3.0±0.3 branches, n=12, p<0.001; Fig. 2B). Second, both pre- and postsynaptic areas were restored to control levels (ex. HRP junctional area - GS +E: 255±16 $\mu m^2$ vs. GS+RU486 0.5 μg/mL: 150±7 $\mu m^2$, n=12, p<0.001; Fig. 2C, D). Finally, the over-proliferation of synaptic boutons was rescued for both the large, mature boutons (GS +E: 28±1 boutons vs. GS+RU486 0.5 μg/mL: 17±1 boutons, n=12, p<0.001; Fig. 2F) and the small, immature satellite boutons (GS+E: 3.4±0.3 mini-boutons vs. GS+RU486 0.5 μg/mL: 0.3±0.1 mini-boutons, n=12, p<0.001; Fig. 2G). These findings demonstrate an entirely presynaptic requirement for dFMRP in synaptic structuring.

### Temporal control of dFMRP expression in the nervous system

Having confirmed GS system utility for examining morphological rescue strategies, we next moved to presynaptic dFMRP induction during discrete temporal windows. To test developmental roles in establishment of synaptic organization, early GS induction of dFMRP was first examined. GS animals were treated with RU486 within 3 hours of hatching for a brief period of 12 hours (Fig. 3A). Neuronal dFMRP levels were then immediately analyzed for comparison relative to wild-type control (Fig. 3B). RU486 fed at 0.1 μg/mL yielded dFMRP levels closest to control at 142±48%, whereas higher concentrations induced steep, dosage dependent over-expression (0.25 μg/mL: 397±128% and 0.5 μg/mL: 556±268%; Fig. 3C).

The duration of dFMRP expression was analyzed by monitoring dFMRP levels at timed periods following withdrawal of RU486 (Fig. 3D). At 24 hours post-treatment, there was ~70% reduction relative to initial induced dFMRP level, irrespective of RU486 dosage (RU486 at 0.1 μg/mL: 45±23% and RU486 at 0.25 μg/mL: 107±17% compared to control; Fig. 3E). Loss of dFMRP was progressive, with levels after RU486 treatment at 0.1 μg/mL declining to 35 ±8% at 48 hours, 10±2% at 60 hours and undetectable by 72 hours post-treatment (Fig. 3E). These studies indicate that dFMRP can be rapidly and strongly induced within hours, but that the inherent stability of dFMRP causes persistence during a period of gradual decline. Analysis of normalized dFMRP:α-tubulin intensity values indicate the apparent dFMRP half-life to be

25.5±1.7 hours. This measured relative stability of dFMRP therefore limits the resolution of temporal expression windows.

### Early dFMRP induction fully rescues *dfmr1* null synaptic structure defects

Both FraX patients and *FMR1* KO mice display an increased number of immature-appearing synaptic spines, similar to those occurring during neocortical development (Comery et al., 1997; Galvez and Greenough, 2005; Hinton et al., 1991; Irwin et al., 2001; Nimchinsky et al., 2001; Rudelli et al., 1985). In mutant mice, these aberrant synapses are developmentally transient and disappear, but then reappear later in the mature animal (Galvez and Greenough, 2005; Nimchinsky et al., 2001). These developmental dynamics suggest specific functions for FMRP during defined windows, especially early in synaptogenesis. To test this hypothesis in our model, dFMRP expression was induced for a brief 12 hour window immediately following hatching (Fig. 3A) and mature 3$^{rd}$ instar larvae were collected 72 hours post-treatment (~108 hours after egg lay; AEL), with NMJ synapses co-labeled for HRP and DLG to compare RU486 treated and EtOH control (Fig. 4A). RU486 concentrations of 0.1 μg/mL and 0.25 μg/mL were both analyzed, representing normal and over-expression levels.

Significant and complete rescue of the *dfmr1* null structural phenotypes was observed with transient early expression (Fig. 4B-E). The synaptic over-branching characteristic of *dfmr1* null was fully rescued at the higher dFMRP level (GS+EtOH: 4.8±0.2 branches, n=14 vs. GS +RU486 0.25 μg/mL: 3.4±0.1 branches, n=12, $p<0.001$; Fig. 4B). The greater synaptic bouton number was similarly restored to wild-type level (GS+EtOH: 27±1 boutons, n=14 vs. both GS +RU486 0.1 μg/mL and GS+RU486 0.25 μg/mL: 21±1 boutons, n=12, $p<0.01$; Fig. 4C). Finally, increased synaptic junction area was rescued by both dFMRP levels; for example, the HRP presynaptic area was comparable under both conditions (GS+EtOH: 206±8 $\mu m^2$, n=14 vs. both GS+RU486 0.1 μg/mL: 163±8 $\mu m^2$, n=12, $p<0.01$ and GS+RU486 0.25 μg/mL: 178 ±7 $\mu m^2$, n=12, $p<0.05$; Fig. 4D, E). These findings indicate a specific early developmental requirement for dFMRP in sculpting synaptic architecture. Further, the persistence of normal synaptic structure at the mature NMJ in the absence of dFMRP suggests it is not required for maintenance or stability of synaptic structure once established.

### Late intervention partially restores *dfmr1* null synaptic structure defects

A critical question for FraX patients is whether late correction of the FMRP deficit can ameliorate disease symptoms. Having identified the early role for dFMRP in establishment of NMJ synaptic morphology, we therefore next examined whether reintroduction of dFMRP in mature animals could rescue synapse structural defects. GS animals were treated with either RU486 or EtOH for 12 hours at a mature larval time point (96-108 hrs AEL; Fig. 5A) and then immediately analyzed. Protein level comparisons show that RU486 fed at 1-2 μg/mL drives dFMRP levels that are indistinguishable from wild-type control (99±9% and 90±6%, respectively), whereas RU486 at 5 μg/mL elevates dFMRP to 227±21% of control (compared to both 1 and 2 μg/mL, $p<0.01$ and $p<0.001$, respectively; Fig. 5B,C). Both the low (1 μg/mL) and high (5 μg/mL) RU486 induction levels were used to examine the effect on synaptic architecture.

Examination of NMJ structure following late intervention showed slight but significant rescue of a subset of defects (Fig. 5D). There was no rescue of either branching or synapse area (data not shown). However, the increased synaptic bouton number (GS+EtOH: 27±1 boutons, n=12) was significantly reduced following the 12 hour acute intervention (GS+RU486 1μg/mL: 22 ±1 boutons, n=12 and GS+RU486 5 μg/mL: 23±1 boutons, n=11, $p<0.01$; Fig. 5E). Thus, there is weak, partial rescue of synaptic structural phenotypes mediated by late intervention using the GS system to induce targeted presynaptic dFMRP. This finding indicates both maintained

morphological plasticity at the NMJ synapse and at least modest reversal potential for specific mutant phenotypes.

## Presynaptic dFMRP expression rescues *dfmr1* synaptic cytoskeleton defects

In addition to synaptic architecture, we examined the synaptic organization of the known dFMRP target Futsch, the microtubule-associated MAP1B homolog (Hummel et al., 2000). Futsch is negatively regulated by dFMRP, and *dfmr1; futsch* double mutants display normal NMJ architecture (Zhang et al., 2001). Futsch is required for dendritic, axonal and synaptic development (Bettencourt da Cruz et al., 2005; Roos et al., 2000; Ruiz-Canada et al., 2004). In wandering 3$^{rd}$ instar larvae, null *dfmr1* synapses contain significantly elevated numbers of Futsch-positive, cytoskeletal loops within synaptic boutons (control: 2.0±0.4 loops, n=11 vs. *dfmr1*: 4.3±0.4 loops, n=12, $p<0.001$; Fig. 6A, B). In control animals, the loop structures are usually restricted to terminal boutons. In contrast, *dfmr1* null NMJs display Futsch loop structures abnormally interspersed throughout the entire synaptic arbor (Fig. 6A). GS vehicle-fed animals phenocopy *dfmr1* null, and the defect is partially rescued by constitutively expressing dFMRP (GS+EtOH: 4.7±0.2 loops, n=12 vs. both GS+RU486 0.5 μg/mL: 3.5±0.4 loops, n=12, $p<0.05$ and GS+RU486 2 μg/mL: 3.2±0.3 loops, n=13, $p<0.01$; Fig. 6B).

Examining temporal windows of GS intervention, we observed that 12 hour RU486 treatment at either early or mature larval time point restored a more normal cytoskeletal arrangement examined at 108 hours AEL. In the early treatment window, complete rescue was observed only at the higher RU486 dosage (GS+EtOH: 7.8±0.4 loops, n=11 vs. GS+RU486 0.25 μg/mL: 5.2±0.3 loops, n=12, $p<0.001$; Fig. 6C). In the late treatment, progressive rescue was achieved in a dose-dependent manner with both RU486 concentrations tested (GS+EtOH: 8.8 ±0.6 loops, n=15 vs. GS+RU486 1 μg/mL: 6.1±0.2 loops, n=10, $p<0.01$ and 5 μg/mL: 5.8±0.4 loops, n=11, $p<0.001$; Fig. 6C). These findings suggest that the synaptic organization of the Futsch-positive microtubule cytoskeleton remains plastic throughout development and at maturity and that dFMRP has a constitutively significant role in modulating this mechanism.

## Presynaptic dFMRP expression does not rescue *dfmr1* synapse function

We next examined the potential for dFMRP induction to rescue synapse functional properties. Null *dfmr1* NMJ synapses exhibit a ~2-fold increase in neurotransmission strength (Zhang et al., 2001), but it has not been shown whether the change is due to elevated glutamate release or increased glutamate receptor function. To make this distinction, we used the lipophillic styryl dye FM1-43 that incorporates into the presynaptic vesicle pool, so that loss or retention can be visualized to monitor activity-dependent vesicle cycling (Brumback et al., 2004; Fergestad and Broadie, 2001; Rohrbough et al., 2004). After a round of stimulated dye loading and unloading (Fig. 7A), a significantly greater amount of the dye is released from mutant than control (control: 0.46±0.04 unload:load, n=8 vs. *dfmr1*: 0.31±0.04 unload:load, n=8, $p<0.01$; Fig. 7B). The average area assayed per bouton was equivalent (control: 9.3±1.5 $\mu m^2$, n=5 vs. *dfmr1*: 9.2 ±1 $\mu m^2$, n=5), ensuring that the differences observed were due dye cycling rates and not sampling variablity. The average fluorescence intensity unit (FIU) values obtained after loading were comparable (control: 153±6 FIU vs. *dfmr1*: 153±5 FIU, n=5; Fig. 7C), but unloading was more rapid in the mutant (control: 81±7 FIU vs. *dfmr1*: 43±4 FIU, n=5, $p<0.01$; Fig. 7C). Thus, the depressed level of retained dye in *dfmr1* mutants indicates an enhanced rate of vesicle exocytosis and provides a mechanistic explanation for the elevated evoked synaptic transmission (Zhang et al., 2001).

Surprisingly, constitutive presynaptic dFMRP expression provides no rescue of the FM1-43 functional transmission defect in GS animals (GS+EtOH: 0.29±0.02 unload:load, n=13; GS +RU 0.5 μg/mL: 0.30±0.03 unload:load, n=6; GS+RU 2 μg/mL: 0.29±0.01 unload:load, n=9; Fig. 7B). Again, actual fluorescence intensity values illustrate the heightened unloading phase

and the lack of any phenotypic rescue upon GS induction (load - GS+EtOH: 124±8, GS+RU 0.5 μg/mL: 130±12, GS+RU 2 μg/mL: 127±5, n=5; unload - GS+EtOH: 33±4, GS+RU 0.5 μg/mL: 31±2, GS+RU 2 μg/mL: 36±3, n=5 (Fig. 7C). Of note, GS animals under all conditions appeared to load at slightly lower absolute levels; however, only the difference seen between $w^{1118}$ control (153±6) and GS+EtOH (124±8) is statistically significant ($p<0.05$). These findings indicate an apparent postsynaptic requirement for dFMRP, with retrograde signaling control of presynaptic function. They also indicate that dFMRP displays differential spatial requirements in relation to synaptic structure and function.

To further examine functional requirements, two-electrode voltage-clamp (TEVC) recordings were made to monitor miniature excitatory junctional currents (mEJCs), as a direct measure of glutamate release (Fig. 8A). The mEJC amplitude was comparable between all genotypes, with a modest difference between control (1.01±0.04 nA, n=10) and *dfmr1* null (0.84±0.04 nA, n=10, $p<0.05$; Fig. 8B). In contrast, substantial differences were observed in mEJC frequency, with a nearly 3-fold increase in the *dfmr1* null compared to control (control: 1.2 ±0.2 Hz vs. *dfmr1*: 3.4±0.5 Hz, n=10, $p<0.01$; Fig. 8C). Elevated mEJC frequencies were also present in the GS animals (GS+EtOH: 2.6±0.2 Hz, n=10), and upon presynaptic dFMRP induction, the condition is markedly exacerbated, not rescued toward control (GS+RU 0.5 μg/mL: 5.0±0.7 Hz; GS+RU 2 μg/mL: 6.4±0.9 Hz, n=10; Fig. 8C). These findings provide strong support for a postsynaptic dFMRP requirement in regulating synapse function.

## Discussion

Fragile X Syndrome (FraX) is caused by the loss of FMRP; however, the spatial and temporal requirements for FMRP are largely unknown. The definition of these requirements in nervous system connectivity, transmission and plasticity is critical for understanding FraX pathophysiology and informing the design of effective FraX therapeutic intervention strategies. In this study, we tackle these questions using the established *Drosophila* FraX model, focusing on the NMJ model synapse. We use the inducible Gene-Switch system to control spatial and temporal dFMRP expression in an otherwise null mutant. We show that constitutively expressed presynaptic dFMRP fully rescues synapse architecture and cytoskeleton patterning, but does not restore normal synaptic function. We therefore conclude that dFMRP has critical presynaptic roles controlling synaptic morphology; however, the regulation of neurotransmission strength is mediated by postsynaptic function. We demonstrate that a brief dFMRP pulse early in development is sufficient to meet presynaptic needs controlling synapse configuration, but that a brief pulse at maturity also partially restores normal synapse structure. We therefore conclude that dFMRP plays a primary role early in synapse assembly, but the synapse maintains morphological plasticity. Moreover, late dFMRP reintroduction has some ability to counteract the effects of dFMRP loss throughout development. These conclusions suggest that FraX interventions should be targeted to young children in order to maximize efficacy, but also that restoration, or perhaps circumvention, of FMRP function at maturity could also be beneficial as a FraX treatment strategy.

### Spatial Requirements for FMRP: Presynaptic versus Postsynaptic Function

Although neurological consequences are readily identifiable in the FraX disease state, the causative spatial defects associated with FMRP loss are largely undefined. The most studied structural anomaly in FraX patients and *FMR1* KO mice is increased density of morphologically immature dendritic spines (Comery et al., 1997; Galvez and Greenough, 2005; Hinton et al., 1991; Irwin et al., 2001; Nimchinsky et al., 2001; Rudelli et al., 1985). Although this is commonly treated as a solely postsynaptic defect, spines are synaptic contacts, by definition, so there should be an equivalent defect in opposing presynaptic boutons. Thus, the FMRP requirement could be presynaptic, postsynaptic or both. *Drosophila FMR1* mutants

similarly display synaptic architecture defects in several classes of neurons, including motoneurons (Zhang et al., 2001), lateral and dorsal cluster neurons (Morales et al., 2002), and Mushroom Body Kenyon Cells, a site of learning and memory consolidation (Michel et al., 2004; Pan et al., 2004). At the NMJ, synaptic defects have been attributed to both pre- and postsynaptic roles of dFMRP, as both neuronal and muscle over-expression result in altered architecture (Zhang et al., 2001).

Functionally, the *FMR1* KO mouse displays decreased cortical long-term potentiation (LTP) (Larson et al., 2005; Li et al., 2002) and increased hippocampal long-term depression (LTD) (Huber et al., 2002; Nosyreva and Huber, 2006). The LTD alteration is suggested to be postsynaptically mediated due to FMRP normally functioning to suppress translation of dendritic mRNAs to attenuate LTD (Bear et al., 2004); however, no spatial dissection of this function has been reported. In *Drosophila*, loss of dFMRP results in altered neurotransmission in both visual system synapses and at the NMJ (Zhang et al., 2001). In the most-studied NMJ location, elevated neurotransmission has been suggested to be primarily due to a presynaptic role for dFMRP, as neuronal over-expression results in dramatic elevation in spontaneous vesicle fusion events (Zhang et al., 2001). However, variability in functional outputs may reflect differential FMRP roles in transsynaptic signaling, and decreased postsynaptic sensitivity is often offset by a compensatory increase in presynaptic release (Davis et al., 1998; Frank et al., 2006; Paradis et al., 2001; Petersen et al., 1997; Plomp et al., 1992; Sandrock et al., 1997).

The current study clearly demonstrates a presynaptic role for dFMRP in regulating NMJ synaptic architecture, including terminal area, synaptic branching, and the formation of synaptic boutons; all of which are negatively regulated by dFMRP function in the presynaptic cell. Perhaps most interesting is the accumulation of mini/satellite-boutons in the absence of presynaptic dFMRP function. Work by us and others has suggested that these tiny boutons represent a developmentally-arrested state at an otherwise normal stage of bouton maturation (Ashley et al., 2005; Beumer et al., 1999; Dickman et al., 2006; Torroja et al., 1999). Since the *dfmr1* null also shows a supernumerary abundance of mature synaptic boutons, the accumulation of mini-boutons suggests that absence of presynaptic dFMRP function triggers the initiation of a disproportionate number of bouton formation events, but that other proteins required for bouton maturation are limiting. Therefore, dFMRP has a primary role in restricting bouton deposition. An early-development pulse of dFMRP prevents the aberrant accumulation of mature boutons, but does not prevent accumulation of mini-boutons. Thus, dFMRP is constitutively required in the presynaptic cell to arrest this nascent stage of synaptic bouton formation.

We established previously that dFMRP acts as a translational repressor of the MAP1B homolog Futsch (Zhang et al., 2001). Null *dfmr1* phenotypes are mimicked by presynaptic over-expression of Futsch, and genetic control of Futsch over-expression in the *dfmr1* null background completely rescues NMJ overgrowth phenotypes. Subsequent mouse studies revealed the same MAP1B upregulation and associated enhanced microtubule stability in *FMR1* KO neurons (Lu et al., 2004). At the *Drosophila* NMJ, Futsch binds microtubule hairpin loops in a dynamic subset of synaptic boutons (Roos et al., 2000). In other systems, the appearance of these microtubule structures is linked to the stalling of axonal growth cones (Dent and Kalil, 2001; Tanaka and Kirschner, 1991; Tsui et al., 1984), which predicts a similar role in synapse growth (Roos et al., 2000). In *dfmr1* nulls, however, there is an increased number of Futsch loops throughout the overgrown NMJ synaptic arbor, a defect rescued by targeted presynaptic dFMRP expression. Furthermore, developmental analyses reveal that Futsch loops are more abundant during earlier stages of synapse assembly than at maturity (compare larvae at 108 hours AEL vs. wandering 3$^{rd}$ instars). In *dfmr1* nulls, Futsch loops are significantly more abundant both during active synapse growth as well as at maturity. These results suggest

that the dynamic growth capacity of the synapse is reflected by the number of Futsch loops as a function of developmental time, and thus, that *dfmr1* mutants are arrested in a premature growth state.

Presynaptic induction of dFMRP totally fails to rescue the elevated cycling of synaptic vesicles in the *dfmr1* null mutant, indicating that this defect has its origin in a postsynaptic function of dFMRP. The known postsynaptic function at the *Drosophila* NMJ is selection of the appropriate glutamate receptor classes, with relative abundances dramatically skewed by the absence of dFMRP (Pan and Broadie, 2007). Therefore, our results suggest that defects in the postsynaptic glutamate receptor field cause a compensatory change in the presynaptic vesicle cycling underlying glutamate release, presumably via a transsynaptic retrograde signal (Davis et al., 1998; Frank et al., 2006; Paradis et al., 2001; Petersen et al., 1997). In support of this hypothesis, a recent study showed presynaptic *FMR1* genotype influences synaptic connectivity in a mosaic mouse model, with neurons lacking FMRP less likely to form functional synapses (Hanson and Madison, 2007). Conversely, acute postsynaptic expression of FMRP in *FMR1* KO neurons results in a decrease in the number of functional and structural synapses relative to neighboring untransfected neurons, indicating phenotypic rescue (Pfeiffer and Huber, 2007). While it is possible that pre- and postsynaptic effects are independent of one another, transsynaptic compensation warrants consideration in dissecting the spatial requirement of FMRP in modulating synaptic function.

## Temporal Requirements for FMRP: Development versus Plasticity

In mice, the appearance of *FMR1* mutant phenotypes is age-dependent with at least some defects appearing transiently. In layer V barrel cortex, KO neurons display abnormal dendritic spine length/density during cortical synaptogenesis early in development (postnatal week 1); however, these differences are undetectable by week 4 (Galvez and Greenough, 2005; Nimchinsky et al., 2001). Functionally, mutant mice display brain-region specific defects in both LTD and LTP (Huber et al., 2002; Larson et al., 2005; Li et al., 2002; Nosyreva and Huber, 2006; Wilson and Cox, 2007). However, it is important to realize that such defects may reflect either an acute FMRP function in the adult animal or, just as easily, a transient role of FMRP during development that pre-establishes the ability of synapses to manifest plasticity at maturity. Indeed, synaptic plasticity defects appear to be much more severe during transient developmental windows, with less severe defects at maturity (Huang et al., 2006).

The Gene-Switch system allows rapid induction of dFMRP transcription, but an inherent limitation to the approach rests with the protein half-life. We show here that the dFMRP protein appears relatively stable, with a half-life of ~26 hours. Thus, we can switch “on” dFMRP within a few hours, but the switch “off” is governed by the protein decay profile over the course of several days, limiting temporal resolution. For this reason, we restricted analyses to two intervention windows. First, we employed a 12 hour induction immediately after hatching, carefully determining the induction strength to ensure a match with endogenous dFMRP protein levels. With this treatment, dFMRP levels decrease exponentially with time; the protein was almost undetectable by ~60 hours post-treatment. Second, a brief 12 hour induction at the terminal endpoint of larval life was executed. Again, we carefully controlled induction specific to this mature time point, to match levels of the introduced protein to dFMRP levels in control. With this protocol, the animal completely lacked all dFMRP throughout development with acute protein reintroduction immediately prior to analysis at maturity.

In the early induction paradigm, transient dFMRP expression yields almost complete rescue of *dfmr1* null synaptic structural defects, including expansion of the synaptic terminal area, over-branching of synaptic processes, and the formation of excess synaptic boutons. The resolution towards wild-type architecture indicates a primarily early role for dFMRP in molding the NMJ and suggests that dFMRP-mediated imprinting/patterning of synaptic

development allows for appropriate and sustainable synaptic structure. These findings support the conclusion that dFMRP is required early for proper initiation of synaptogenesis and not synaptic maintenance. This conclusion is perhaps not unexpected for a protein that acts as a translational regulator of synaptogenic proteins, which will have their own perdurance at the synapse once properly regulated by early dFMRP function. In addition, however, acute dFMRP induction at maturity provides partial rescue of synaptic architecture defects. This effect is a true rescue, i.e. resolution of overgrowth phenotypes that are fully manifest at the start of transgene expression window. This finding demonstrates that the established NMJ synapse displays morphological plasticity and can be remodeled. These findings are in agreement with presynaptically-mediated remodeling in which synapse retraction occurs, trailing a postsynaptic "footprint" (Eaton et al., 2002; Pielage et al., 2005). Such regression would be requisite in mediating the observed rescue of *dfmr1* overgrowth via bouton destabilization and elimination.

Much work continues to be focused on alleviating FraX symptoms and targeting the causative molecular insults resulting in the disease state. Recent work in the *FMR1* KO mouse has shown rescue, at cellular and behavioral levels, via constitutive reduction in mGluR5 (Dolen et al., 2007) and p21-activated kinase (Hayashi et al., 2007). Translation of these exciting new findings into clinical treatments will be better informed with the temporal requirement of FMRP clearly defined. In future work, we will test the efficacy of targeted temporal interventions in both mGluR-mediated signaling upstream of FMRP function as well as translational consequences downstream of FMRP function.

## Acknowledgements

We are especially grateful to Dr. Haig Keshishian (Yale University) for the *elav*-Gene-Switch line that made this work possible. We thankfully acknowledge the *Drosophila* Bloomington Stock Center and the Iowa Developmental Studies Hybridoma Bank for essential genetic lines and antibodies, respectively. We would like to acknowledge Dr. Elisabeth Dykens (Vanderbilt Kennedy Center for Research on Human Development) for her role in providing clinical co-mentorship to C.G. during this project. We give thanks to members of the Broadie Lab, especially Dr. Charles Tessier, for insightful discussion. We would also like to extend our gratitude to Drs. Sarah Repicky, Jeffrey Rohrbough and Kevin Haas, and Ms. Ashleigh Long for technical training, suggestions and support with regard to the electrophysiology studies presented. This work has been funded by the National Institutes of Health through the NIH Roadmap for Medical Research Training Grant T32 MH075883 to C.G. and R01 grant GM54544 to K.B.

## References

Antar LN, Afroz R, Dictenberg JB, Carroll RC, Bassell GJ. Metabotropic glutamate receptor activation regulates fragile x mental retardation protein and FMR1 mRNA localization differentially in dendrites and at synapses. J Neurosci 2004;24:2648–55. [PubMed: 15028757]

Ashley J, Packard M, Ataman B, Budnik V. Fasciclin II signals new synapse formation through amyloid precursor protein and the scaffolding protein dX11/Mint. J Neurosci 2005;25:5943–55. [PubMed: 15976083]

Bailey DB Jr. Hatton DD, Skinner M, Mesibov G. Autistic behavior, FMR1 protein, and developmental trajectories in young males with fragile X syndrome. J Autism Dev Disord 2001a;31:165–74. [PubMed: 11450815]

Bailey DB Jr. Hatton DD, Tassone F, Skinner M, Taylor AK. Variability in FMRP and early development in males with fragile X syndrome. Am J Ment Retard 2001b;106:16–27. [PubMed: 11246709]

Bear MF, Huber KM, Warren ST. The mGluR theory of fragile X mental retardation. Trends Neurosci 2004;27:370–7. [PubMed: 15219735]

Bettencourt da Cruz A, Schwarzel M, Schulze S, Niyyati M, Heisenberg M, Kretzschmar D. Disruption of the MAP1B-related protein FUTSCH leads to changes in the neuronal cytoskeleton, axonal transport defects, and progressive neurodegeneration in Drosophila. Mol Biol Cell 2005;16:2433–42. [PubMed: 15772149]

Beumer KJ, Rohrbough J, Prokop A, Broadie K. A role for PS integrins in morphological growth and synaptic function at the postembryonic neuromuscular junction of Drosophila. Development 1999;126:5833–46. [PubMed: 10572057]

Brumback AC, Lieber JL, Angleson JK, Betz WJ. Using FM1-43 to study neuropeptide granule dynamics and exocytosis. Methods 2004;33:287–94. [PubMed: 15183177]

Castets M, Schaeffer C, Bechara E, Schenck A, Khandjian EW, Luche S, Moine H, Rabilloud T, Mandel JL, Bardoni B. FMRP interferes with the Rac1 pathway and controls actin cytoskeleton dynamics in murine fibroblasts. Hum Mol Genet 2005;14:835–44. [PubMed: 15703194]

Comery TA, Harris JB, Willems PJ, Oostra BA, Irwin SA, Weiler IJ, Greenough WT. Abnormal dendritic spines in fragile X knockout mice: maturation and pruning deficits. Proc Natl Acad Sci U S A 1997;94:5401–4. [PubMed: 9144249]

Cornish KM, Munir F, Cross G. Differential impact of the FMR-1 full mutation on memory and attention functioning: a neuropsychological perspective. J Cogn Neurosci 2001;13:144–50. [PubMed: 11224914]

Davis GW, DiAntonio A, Petersen SA, Goodman CS. Postsynaptic PKA controls quantal size and reveals a retrograde signal that regulates presynaptic transmitter release in Drosophila. Neuron 1998;20:305–15. [PubMed: 9491991]

Dent EW, Kalil K. Axon branching requires interactions between dynamic microtubules and actin filaments. J Neurosci 2001;21:9757–69. [PubMed: 11739584]

Dickman DK, Lu Z, Meinertzhagen IA, Schwarz TL. Altered synaptic development and active zone spacing in endocytosis mutants. Curr Biol 2006;16:591–8. [PubMed: 16546084]

Dockendorff TC, Su HS, McBride SM, Yang Z, Choi CH, Siwicki KK, Sehgal A, Jongens TA. Drosophila lacking dfmr1 activity show defects in circadian output and fail to maintain courtship interest. Neuron 2002;34:973–84. [PubMed: 12086644]

Dolen G, Osterweil E, Rao BS, Smith GB, Auerbach BD, Chattarji S, Bear MF. Correction of Fragile X Syndrome in Mice. Neuron 2007;56:955–962. [PubMed: 18093519]

Eaton BA, Fetter RD, Davis GW. Dynactin is necessary for synapse stabilization. Neuron 2002;34:729–41. [PubMed: 12062020]

Einfeld S, Hall W, Levy F. Hyperactivity and the fragile X syndrome. J Abnorm Child Psychol 1991;19:253–62. [PubMed: 1865044]

Fergestad T, Broadie K. Interaction of stoned and synaptotagmin in synaptic vesicle endocytosis. J Neurosci 2001;21:1218–27. [PubMed: 11160392]

Ferrari F, Mercaldo V, Piccoli G, Sala C, Cannata S, Achsel T, Bagni C. The fragile X mental retardation protein-RNP granules show an mGluR-dependent localization in the post-synaptic spines. Mol Cell Neurosci 2007;34:343–54. [PubMed: 17254795]

Frank CA, Kennedy MJ, Goold CP, Marek KW, Davis GW. Mechanisms underlying the rapid induction and sustained expression of synaptic homeostasis. Neuron 2006;52:663–77. [PubMed: 17114050]

Galvez R, Greenough WT. Sequence of abnormal dendritic spine development in primary somatosensory cortex of a mouse model of the fragile X mental retardation syndrome. Am J Med Genet A 2005;135:155–60. [PubMed: 15880753]

Gould EL, Loesch DZ, Martin MJ, Hagerman RJ, Armstrong SM, Huggins RM. Melatonin profiles and sleep characteristics in boys with fragile X syndrome: a preliminary study. Am J Med Genet 2000;95:307–15. [PubMed: 11186882]

Hanson JE, Madison DV. Presynaptic FMR1 genotype influences the degree of synaptic connectivity in a mosaic mouse model of fragile X syndrome. J Neurosci 2007;27:4014–8. [PubMed: 17428978]

Hayashi ML, Rao BS, Seo JS, Choi HS, Dolan BM, Choi SY, Chattarji S, Tonegawa S. Inhibition of p21-activated kinase rescues symptoms of fragile X syndrome in mice. Proc Natl Acad Sci U S A 2007;104:11489–94. [PubMed: 17592139]

Hinton VJ, Brown WT, Wisniewski K, Rudelli RD. Analysis of neocortex in three males with the fragile X syndrome. Am J Med Genet 1991;41:289–94. [PubMed: 1724112]

Huang Z, Shimazu K, Woo NH, Zang K, Muller U, Lu B, Reichardt LF. Distinct roles of the beta 1-class integrins at the developing and the mature hippocampal excitatory synapse. J Neurosci 2006;26:11208–19. [PubMed: 17065460]

Huber KM, Gallagher SM, Warren ST, Bear MF. Altered synaptic plasticity in a mouse model of fragile X mental retardation. Proc Natl Acad Sci U S A 2002;99:7746–50. [PubMed: 12032354]

Hummel T, Krukkert K, Roos J, Davis G, Klambt C. Drosophila Futsch/22C10 is a MAP1B-like protein required for dendritic and axonal development. Neuron 2000;26:357–70. [PubMed: 10839355]

Inoue S, Shimoda M, Nishinokubi I, Siomi MC, Okamura M, Nakamura A, Kobayashi S, Ishida N, Siomi H. A role for the Drosophila fragile X-related gene in circadian output. Curr Biol 2002;12:1331–5. [PubMed: 12176363]

Irwin SA, Patel B, Idupulapati M, Harris JB, Crisostomo RA, Larsen BP, Kooy F, Willems PJ, Cras P, Kozlowski PB, et al. Abnormal dendritic spine characteristics in the temporal and visual cortices of patients with fragile-X syndrome: a quantitative examination. Am J Med Genet 2001;98:161–7. [PubMed: 11223852]

Jan LY, Jan YN. Properties of the larval neuromuscular junction in Drosophila melanogaster. J Physiol (Lond) 1976;262:189–214. [PubMed: 11339]

Koukoui SD, Chaudhuri A. Neuroanatomical, molecular genetic, and behavioral correlates of fragile X syndrome. Brain Res Rev 2007;53:27–38. [PubMed: 16844227]

Larson J, Jessen RE, Kim D, Fine AK, du Hoffmann J. Age-dependent and selective impairment of long-term potentiation in the anterior piriform cortex of mice lacking the fragile X mental retardation protein. J Neurosci 2005;25:9460–9. [PubMed: 16221856]

Li J, Pelletier MR, Perez Velazquez JL, Carlen PL. Reduced cortical synaptic plasticity and GluR1 expression associated with fragile X mental retardation protein deficiency. Mol Cell Neurosci 2002;19:138–51. [PubMed: 11860268]

Lu R, Wang H, Liang Z, Ku L, O'Donnell W T, Li W, Warren ST, Feng Y. The fragile X protein controls microtubule-associated protein 1B translation and microtubule stability in brain neuron development. Proc Natl Acad Sci U S A 2004;101:15201–6. [PubMed: 15475576]

McGuire SE, Roman G, Davis RL. Gene expression systems in Drosophila: a synthesis of time and space. Trends Genet 2004;20:384–91. [PubMed: 15262411]

Michel CI, Kraft R, Restifo LL. Defective neuronal development in the mushroom bodies of Drosophila fragile X mental retardation 1 mutants. J Neurosci 2004;24:5798–809. [PubMed: 15215302]

Morales J, Hiesinger PR, Schroeder AJ, Kume K, Verstreken P, Jackson FR, Nelson DL, Hassan BA. Drosophila fragile X protein, DFXR, regulates neuronal morphology and function in the brain. Neuron 2002;34:961–72. [PubMed: 12086643]

Muddashetty RS, Kelic S, Gross C, Xu M, Bassell GJ. Dysregulated metabotropic glutamate receptor-dependent translation of AMPA receptor and postsynaptic density-95 mRNAs at synapses in a mouse model of fragile X syndrome. J Neurosci 2007;27:5338–48. [PubMed: 17507556]

Munir F, Cornish KM, Wilding J. Nature of the working memory deficit in fragile-X syndrome. Brain Cogn 2000;44:387–401. [PubMed: 11104532]

Nimchinsky EA, Oberlander AM, Svoboda K. Abnormal development of dendritic spines in FMR1 knock-out mice. J Neurosci 2001;21:5139–46. [PubMed: 11438589]

Nosyreva ED, Huber KM. Metabotropic receptor-dependent long-term depression persists in the absence of protein synthesis in the mouse model of Fragile X Syndrome. J Neurophysiol. 2006

Osterwalder T, Yoon KS, White BH, Keshishian H. A conditional tissue-specific transgene expression system using inducible GAL4. Proc Natl Acad Sci U S A 2001;98:12596–601. [PubMed: 11675495]

Pan L, Broadie KS. Drosophila fragile X mental retardation protein and metabotropic glutamate receptor A convergently regulate the synaptic ratio of ionotropic glutamate receptor subclasses. J Neurosci 2007;27:12378–89. [PubMed: 17989302]

Pan L, Woodruff E 3rd, Liang P, Broadie K. Mechanistic relationships between Drosophila fragile X mental retardation protein and metabotropic glutamate receptor A signaling. Mol Cell Neurosci. 2008

Pan L, Zhang YQ, Woodruff E, Broadie K. The Drosophila fragile X gene negatively regulates neuronal elaboration and synaptic differentiation. Curr Biol 2004;14:1863–70. [PubMed: 15498496]

Paradis S, Sweeney ST, Davis GW. Homeostatic control of presynaptic release is triggered by postsynaptic membrane depolarization. Neuron 2001;30:737–49. [PubMed: 11430807]

Penagarikano O, Mulle JG, Warren ST. The pathophysiology of fragile x syndrome. Annu Rev Genomics Hum Genet 2007;8:109–29. [PubMed: 17477822]

Petersen SA, Fetter RD, Noordermeer JN, Goodman CS, DiAntonio A. Genetic analysis of glutamate receptors in Drosophila reveals a retrograde signal regulating presynaptic transmitter release. Neuron 1997;19:1237–48. [PubMed: 9427247]

Pfeiffer BE, Huber KM. Fragile X mental retardation protein induces synapse loss through acute postsynaptic translational regulation. J Neurosci 2007;27:3120–30. [PubMed: 17376973]

Pielage J, Fetter RD, Davis GW. Presynaptic spectrin is essential for synapse stabilization. Curr Biol 2005;15:918–28. [PubMed: 15916948]

Plomp JJ, van Kempen GT, Molenaar PC. Adaptation of quantal content to decreased postsynaptic sensitivity at single endplates in alpha-bungarotoxin-treated rats. J Physiol 1992;458:487–99. [PubMed: 1302275]

Reeve SP, Bassetto L, Genova GK, Kleyner Y, Leyssen M, Jackson FR, Hassan BA. The Drosophila fragile X mental retardation protein controls actin dynamics by directly regulating profilin in the brain. Curr Biol 2005;15:1156–63. [PubMed: 15964283]

Rohrbough J, Rushton E, Palanker L, Woodruff E, Matthies HJ, Acharya U, Acharya JK, Broadie K. Ceramidase regulates synaptic vesicle exocytosis and trafficking. J Neurosci 2004;24:7789–803. [PubMed: 15356190]

Roos J, Hummel T, Ng N, Klambt C, Davis GW. Drosophila Futsch regulates synaptic microtubule organization and is necessary for synaptic growth. Neuron 2000;26:371–82. [PubMed: 10839356]

Rudelli RD, Brown WT, Wisniewski K, Jenkins EC, Laure-Kamionowska M, Connell F, Wisniewski HM. Adult fragile X syndrome. Clinico-neuropathologic findings. Acta Neuropathol 1985;67:289–95. [PubMed: 4050344]

Ruiz-Canada C, Ashley J, Moeckel-Cole S, Drier E, Yin J, Budnik V. New synaptic bouton formation is disrupted by misregulation of microtubule stability in aPKC mutants. Neuron 2004;42:567–80. [PubMed: 15157419]

Sabaratnam M, Vroegop PG, Gangadharan SK. Epilepsy and EEG findings in 18 males with fragile X syndrome. Seizure 2001;10:60–3. [PubMed: 11181100]

Sandrock AW Jr. Dryer SE, Rosen KM, Gozani SN, Kramer R, Theill LE, Fischbach GD. Maintenance of acetylcholine receptor number by neuregulins at the neuromuscular junction in vivo. Science 1997;276:599–603. [PubMed: 9110980]

Tanaka EM, Kirschner MW. Microtubule behavior in the growth cones of living neurons during axon elongation. J Cell Biol 1991;115:345–63. [PubMed: 1918145]

Todd PK, Mack KJ, Malter JS. The fragile X mental retardation protein is required for type-I metabotropic glutamate receptor-dependent translation of PSD-95. Proc Natl Acad Sci U S A 2003;100:14374–8. [PubMed: 14614133]

Torroja L, Packard M, Gorczyca M, White K, Budnik V. The Drosophila beta-amyloid precursor protein homolog promotes synapse differentiation at the neuromuscular junction. J Neurosci 1999;19:7793–803. [PubMed: 10479682]

Tsui HT, Lankford KL, Ris H, Klein WL. Novel organization of microtubules in cultured central nervous system neurons: formation of hairpin loops at ends of maturing neurites. J Neurosci 1984;4:3002–13. [PubMed: 6502218]

Wilson BM, Cox CL. Absence of metabotropic glutamate receptor-mediated plasticity in the neocortex of fragile X mice. Proc Natl Acad Sci U S A 2007;104:2454–9. [PubMed: 17287348]

Zalfa F, Eleuteri B, Dickson KS, Mercaldo V, De Rubeis S, di Penta A, Tabolacci E, Chiurazzi P, Neri G, Grant SG, et al. A new function for the fragile X mental retardation protein in regulation of PSD-95 mRNA stability. Nat Neurosci 2007;10:578–87. [PubMed: 17417632]

Zhang YQ, Bailey AM, Matthies HJ, Renden RB, Smith MA, Speese SD, Rubin GM, Broadie K. Drosophila fragile X-related gene regulates the MAP1B homolog Futsch to control synaptic structure and function. Cell 2001;107:591–603. [PubMed: 11733059]

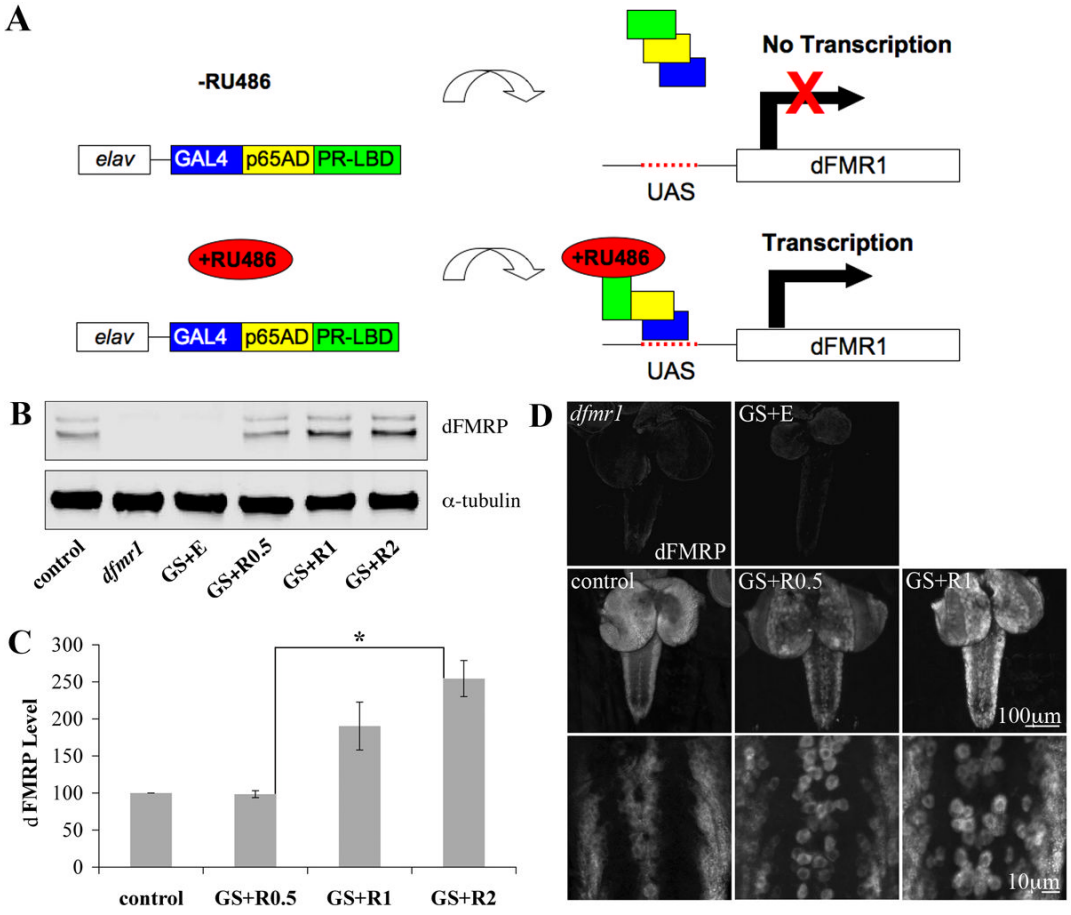


**Figure 1. Gene-Switch system drives targeted dFMRP expression in neurons**

**A)** Cartoon of Gene-Switch system. The GAL4 DNA-binding domain is fused to the p65 activation domain and a mutated progesterone receptor ligand-binding domain. In the absence of RU486, the Gene-Switch is "off." In the presence of RU486, the hormone-responsive GAL4 drives dFMRP transcription downstream of the UAS regulatory sequence. This approach allows spatial and temporal control of dFMRP expression in the *dfmr1* null background. **B)** Western blot of isolated 3rd instar CNS. Genotype as indicated: $w^{1118}$ (control), homozygous $dfmr1^{50M}$ null allele (*dfmr1*) and $dfmr1^{50M}$, *elav*-GSG-301/$dfmr1^{50M}$, UAS-9557-3 (GS). Treatment as indicated: GS fed ethanol vehicle (GS+E) and RU486 at X μg/mL (GS+RX). Blot probed for dFMRP and α-tubulin, illustrating RU486 dosage-responsiveness. **C)** Quantification of western blot dFMRP levels. Individual band intensities were determined normalized to α-tubulin and expressed as percent of control. Bars indicate mean±s.e.m. Significance level: $p<0.05$ (*). **D)** dFMRP immunohistochemistry of wandering 3rd instar CNS. Note RU486 dosage dependence of dFMRP expression.

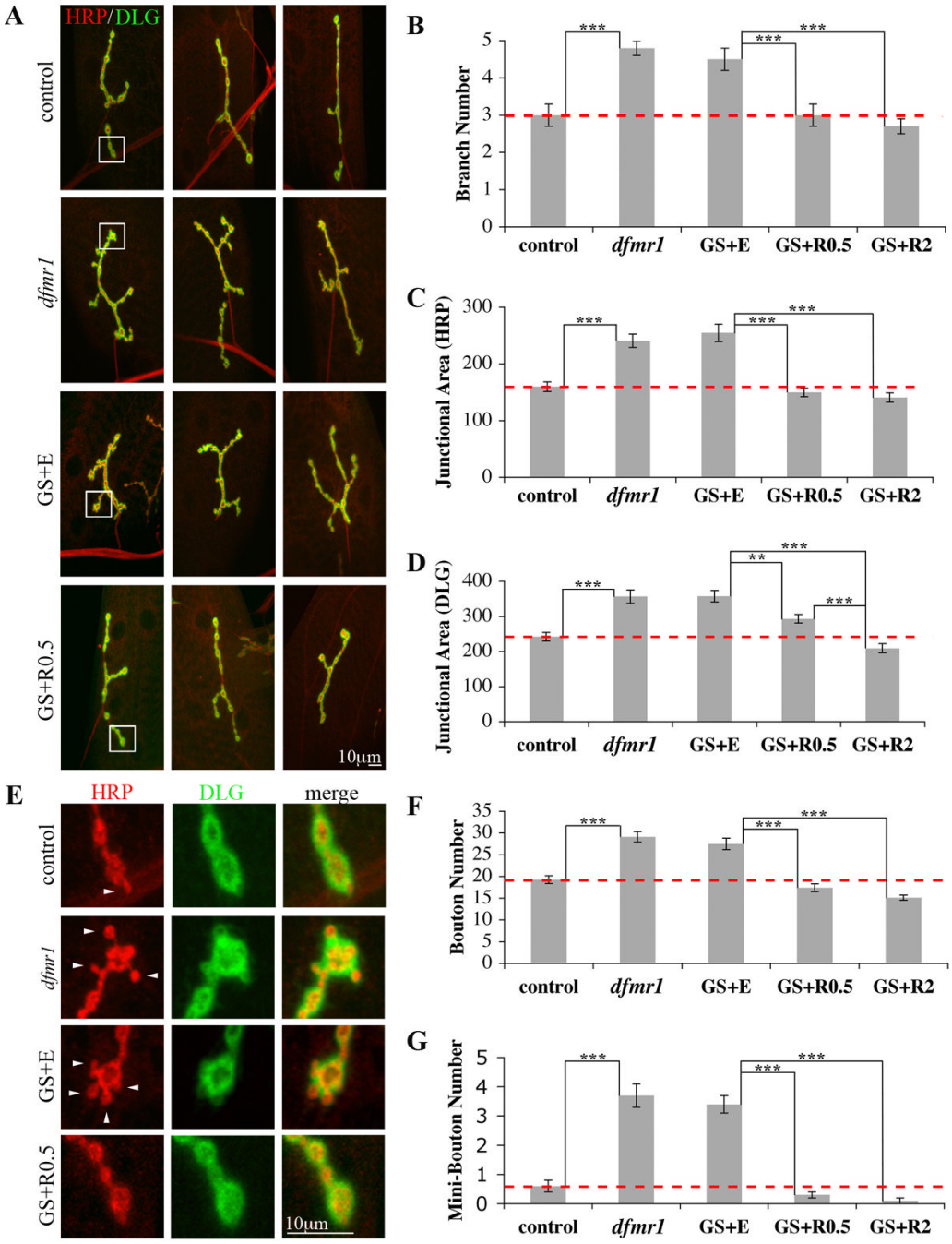


**Figure 2. Targeted presynaptic dFMRP rescues all *dfmr1* NMJ structure defects**

**A)** Representative images of wandering 3rd instar NMJs in genotypes and treatments shown. NMJs co-labeled for HRP (presynaptic marker) and DLG (postsynaptic marker), with three examples of each condition shown. **B-D)** Quantification of NMJ synaptic branch number and area, defined for presynaptic area (HRP domain) and postsynaptic area (DLG domain). Null *dfmr1* terminals display over-growth and over-elaboration. GS+E phenocopies *dfmr1*, and complete rescue occurs with RU486 constitutively driving presynaptic dFMRP expression. **E)** Representative images of mini/satellite boutons in genotypes and treatments shown. High magnification images of boxed regions in (A) showing mini-boutons (arrowheads) in both *dfmr1* and GS+E genotypes and their absence following RU486 induction. **F, G)** Quantification

of normal (>2 μm diameter) and mini-bouton (<2 μm diameter, attached to a normal bouton) number per NMJ in genotypes and treatments shown. n=12 animals for all conditions. Bars indicate mean±s.e.m. Dashed red lines highlight control level quantifications. Significance levels are represented as $p<0.01$ (**) and $p<0.001$ (***).

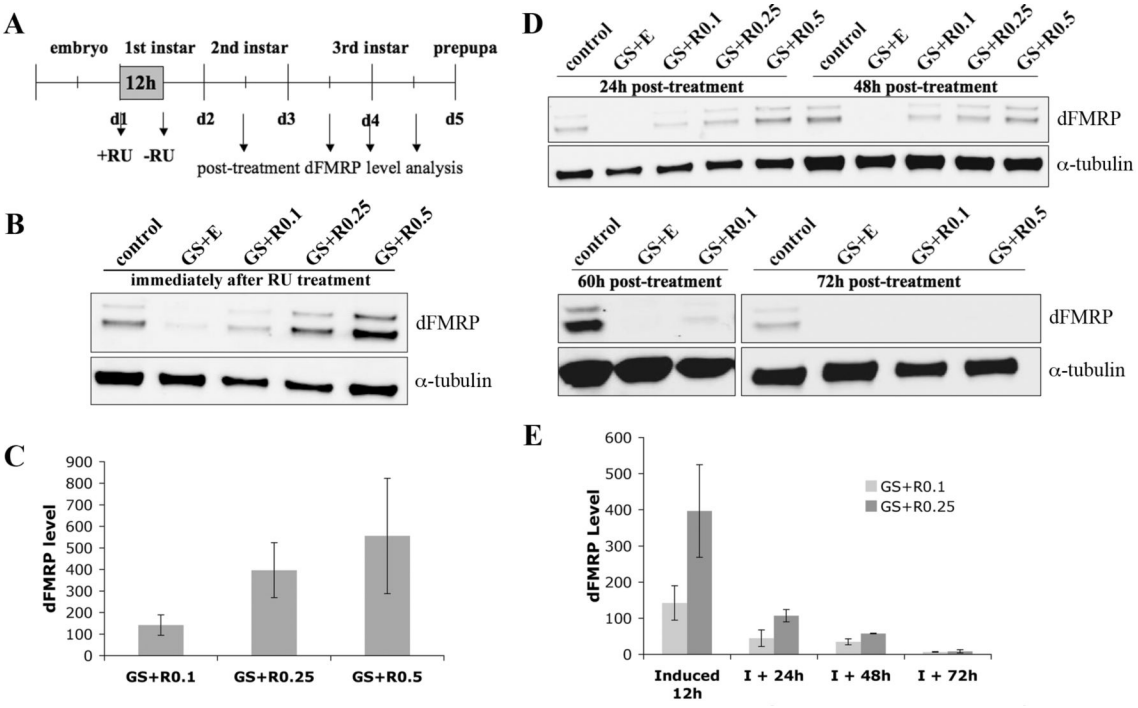


**Figure 3. Temporal control of dFMRP expression by acute early RU486 treatment**

**A)** Depiction of time line employed for early larval induction of dFMRP indicating points of dFMRP protein analyses. **B)** Representative western blot of 1st instar CNS probed for dFMRP and α-tubulin. Samples were taken immediately after 12 hour treatment with RU486 as indicated. **C)** Quantification of western blot dFMRP levels. Individual band intensities were determined normalized to α-tubulin and expressed as percent of control. Bars indicate mean ±s.e.m. **D)** Representative western blots of 2nd and 3rd instar CNS. dFMRP levels progressively diminish and are minimally detectable 60 hours post-treatment. **E)** Quantification of dFMRP levels as a function of age. Individual band intensities were determined normalized to α-tubulin and expressed as percent of control. Bars indicate mean±s.e.m.

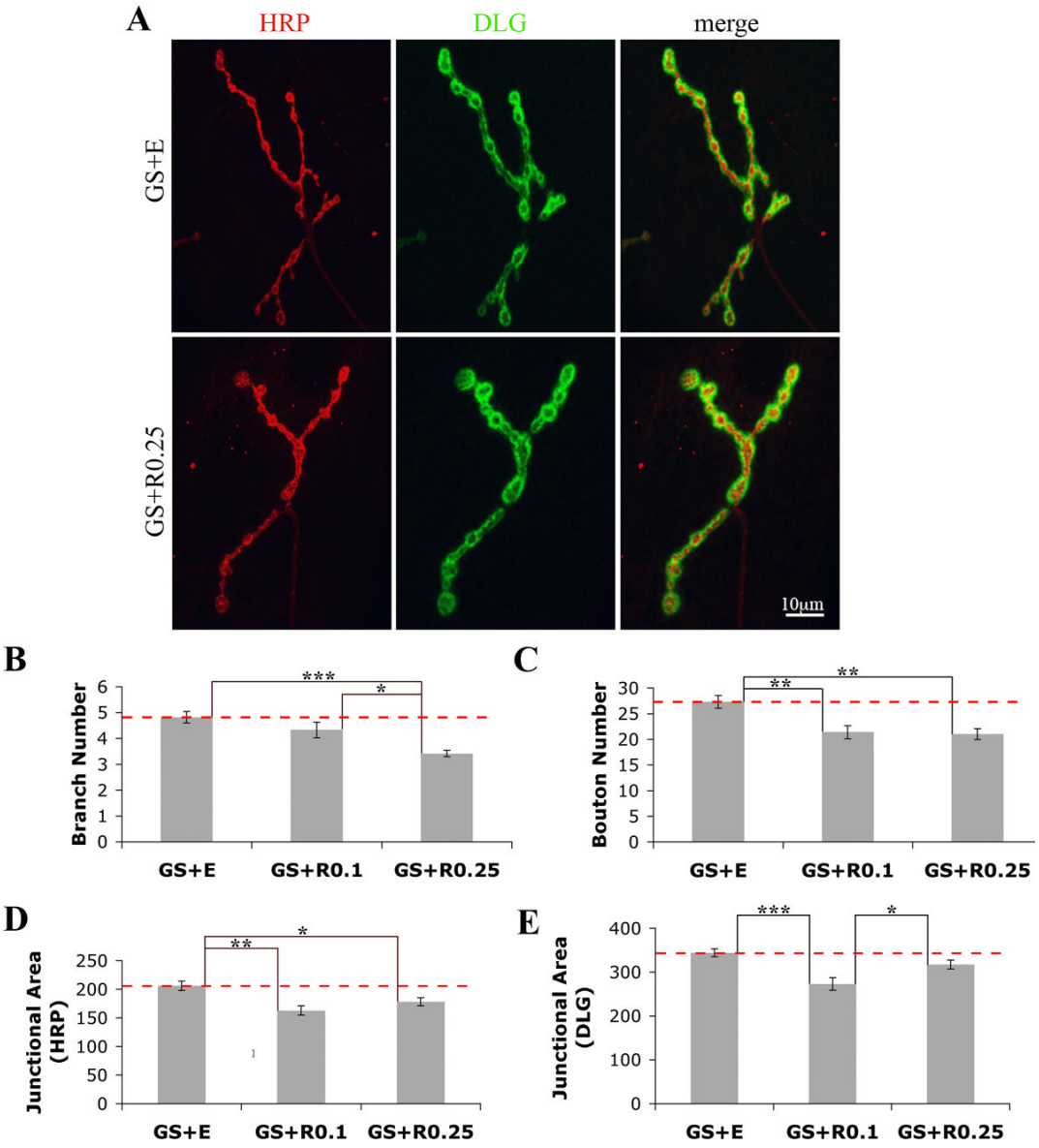


**Figure 4. Early presynaptic dFMRP rescues *dfmr1* NMJ architectural phenotypes**

**A)** Representative images showing NMJs from animals either vehicle- (GS+E) or experimentally treated (GS+RU486 at 0.25 mg/mL, RU+0.25) for 12 hours immediately post-hatching and then analyzed as 3rd instars (108 hours AEL), co-labeled with HRP and DLG. **B-E)** Quantification of NMJ structure. Statistically significant rescue occurs for synaptic branch number (B), synaptic bouton number (C), presynaptic junctional area (D), and postsynaptic junction area (E). n=12-14 animals for each condition. Bars indicate mean±s.e.m. Dashed red lines highlight *dfmr1* null conditions. Significance levels are represented as $p<0.05$ (*); $p<0.01$ (**); $p<0.001$ (***).

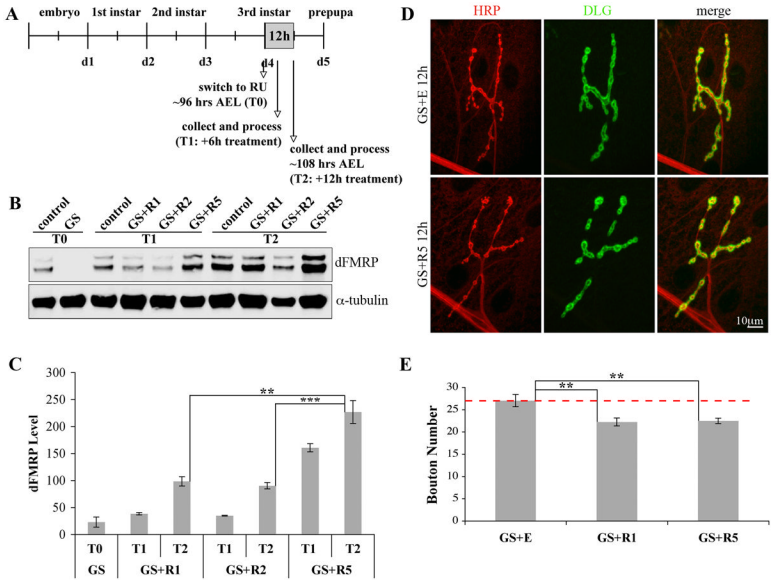


**Figure 5. Acute late presynaptic dFMRP partially rescues *dfmr1* NMJ structure**

**A)** Depiction of time line employed for late larval stage intervention. Larvae were raised to 96 hours AEL, transferred to RU486-containing food for 12 hours, and then immediately processed. **B)** Representative western blot of 3rd instar CNS probed for dFMRP and α-tubulin. **C)** Quantification of western blot dFMRP levels. Individual band intensities were determined normalized to α-tubulin and expressed as percent of control. Bars indicate mean±s.e.m. Significance levels are represented as $p<0.01$ (**) and $p<0.001$ (***). **D)** Representative NMJ images from animals treated during the late 12 hour time period, co-labeled with HRP and DLG. Acute dFMRP expression reduces excess number of boutons observed in the *dfmr1* null. **E)** Quantification of synaptic bouton number. Late 12 hour treatment with RU486 to induce dFMRP effects partial rescue of NMJ structural alterations. n=10-12 animals for each condition. Bars indicate mean±s.e.m. Dashed red line highlights the *dfmr1* null condition. Significance levels are represented as $p<0.01$ (**).

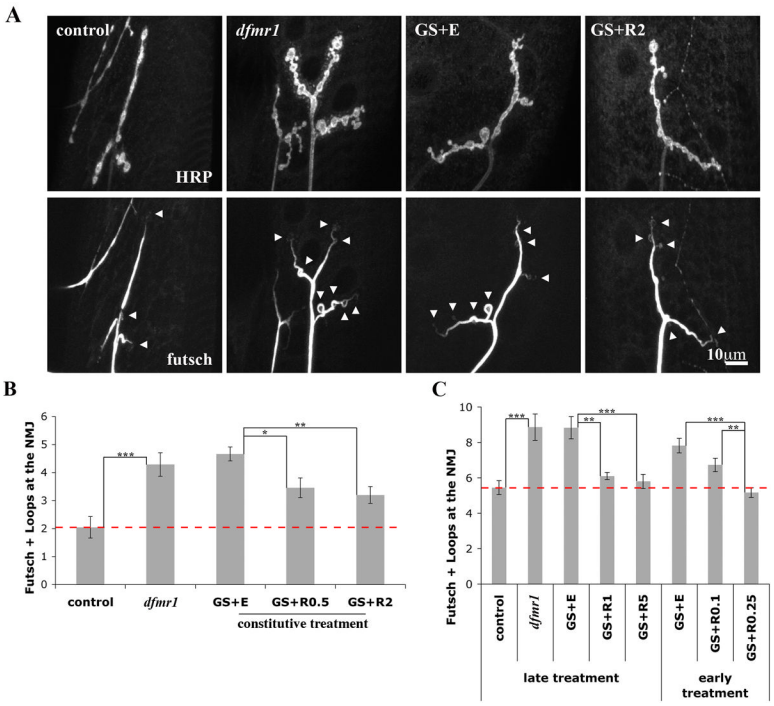


**Figure 6. Targeted presynaptic dFMRP rescue *dfmr1* NMJ cytoskeletal defects**

**A)** Representative images of NMJs from wandering 3rd instars probed for HRP and Futsch/MAP1B. GS animals were constitutively fed either EtOH vehicle or RU486 at 2 μg/mL. Note the increased number of Futsch loops present throughout the *dfmr1* null synaptic terminals. **B)** Quantification of Futsch loops. In wandering 3rd instars, constitutive treatment with RU486 partially rescues the cytoskeletal alteration of null mutant. n=11-13 animals for each condition. **C)** Quantification of futsch loops after either early and late 12 hour treatment with RU486 (taken at 108 hours AEL). Age-matched control and *dfmr1* nulls are presented. n=10-15 animals for each condition. Bars indicate mean±s.e.m. Dashed red line highlights control level quantifications. Significance levels are represented as $p<0.05$ (*); $p<0.01$ (**); $p<0.001$(***).

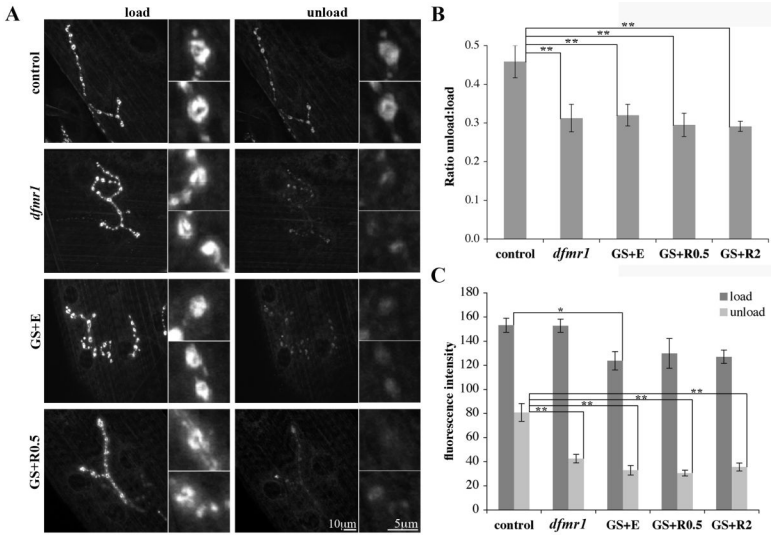


**Figure 7. Constitutive presynaptic dFMRP does not rescue *dfmr1* FM1-43 function defect**

**A)** Representative images of wandering 3rd instar NMJs loaded with FM1-43 and then subsequently unloaded with high $K^+$ depolarizing saline. Note the elevated relative fluorescence retained in control versus *dfmr1* null and GS mutants. Representative synaptic boutons shown at higher magnification. **B)** Quantification of the FM1-43 unload:load fluorescence intensity ratio. Sample sizes: n=8 each control and *dfmr1*; n=13 GS+E, n=6 GS +R0.5, and n=9 GS+RU2. **C**) Quantification of average fluorescence intensity per bouton in loaded and unloaded conditions. Sample sizes: n=5 for each control, *dfmr1*, GS+E, GS+R0.5, and GS+RU2. Bars indicate mean±s.e.m. Significance levels are represented as $p<0.05$ (*), $p<0.01$ (**) and $p<0.01$ (**).

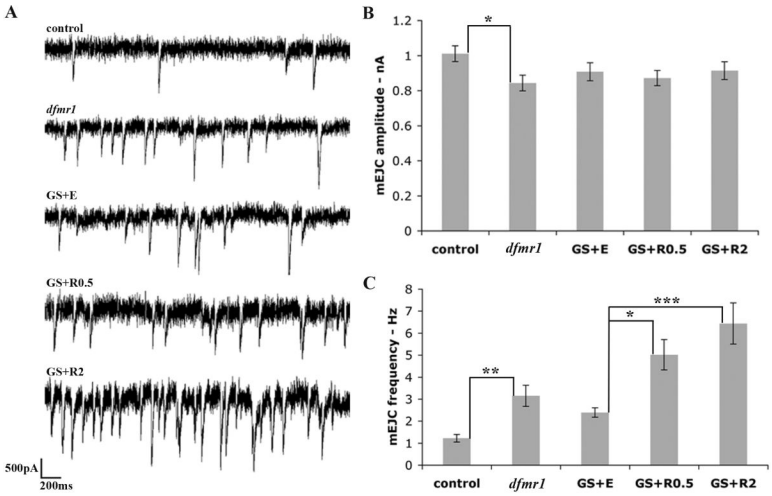


**Figure 8. Constitutive presynaptic dFMRP does not rescue *dfmr1* mEJC function defect**

**A**) Sample mEJC traces from wandering 3rd instar NMJs showing 3 seconds of recording from control, *dfmr1*, GS+E, GS+R0.5, and GS+RU2. Note the increased number of events in *dfmr1* null compared to control, and further increase upon dFMRP induction. **B**) Quantification of mEJC peak amplitude. **C**) Quantification of mEJC frequency. Bars indicate mean±s.e.m; n=10 for each category. Significance levels represented as $p<0.05$ (*); $p<0.01$ (**); $p<0.001$ (***).